

## Aqueous Solution Properties of Polyglycidol-Based Analogues of Pluronic Copolymers. Influence of the Poly(propylene oxide) Block Molar Mass

Silvia Halacheva,<sup>†,‡</sup> Stanislav Rangelov,<sup>\*,†</sup> Christo Tsvetanov,<sup>†</sup> and Vasil M. Garamus<sup>§</sup>

<sup>†</sup>*Institute of Polymers, Bulgarian Academy of Sciences, Acad. G. Bonchev 103-A, 1113 Sofia, Bulgaria,*

<sup>‡</sup>*Physical and Theoretical Chemistry Laboratory, Oxford University, South Parks Road, Oxford OX1 3QZ, U.K., and*

<sup>§</sup>*GKSS Research Centre, Max Planck Strasse 1, D-21502 Geesthacht, Germany*

*Received September 28, 2009; Revised Manuscript Received November 15, 2009*

**ABSTRACT:** With the present contribution we complement the picture of the behavior in aqueous solution of the entire family of LGP copolymers. The latter are considered analogues of the Pluronic copolymers in which the flanking poly(ethylene oxide) (PEO) blocks are substituted by linear polyglycidol (PG). PG is structurally similar to PEO and differs in that each monomer unit bears a hydroxymethylene group. So far two series of LGP copolymers, that is LGP60 and LGP130, based on poly(propylene oxide) (PPO) of molar masses 2000 and 4000, respectively, and PG contents ranging from 10 to 84 wt % have been studied. In particular, in the present paper we report on the synthesis and aqueous solution properties of a novel series of LGP copolymers that are close in composition to the Pluronic copolymers of the lowest molar mass of the central block of PPO, L31–P38. Seven copolymers based on PPO of molar mass of 1000 and PG content ranging from 30 to 90 wt % were prepared by applying the same two-step procedure employed for the synthesis of the LGP60 and LGP130 copolymers. The copolymers were prepared by means of anionic polymerization of ethoxyethyl glycidyl ether (protected glycidol) followed by cleavage of the protective groups. The aqueous solution properties were thoroughly investigated by a variety of methods, e.g., dye solubilization for determination of the critical micellization concentrations, turbidimetry, light scattering, small-angle neutron scattering, and rheology. A number of parameters were extracted from the experimental data and compared to those of the related copolymers from the LGP60 and LGP130 series to assess the influence of the molar mass of the central block of PPO.

### Introduction

Our recent articles on novel polyglycidol–poly(propylene oxide)–polyglycidol (PG–PPO–PG or LGP) triblock copolymers have focused on the synthesis and aqueous solution properties of two series of copolymers.<sup>1,2</sup> These were based nominally on PPO of constant molar masses of 2000 (LGP60 series) and 4000 (LGP130 series) and were prepared in different PG contents covering the range from 10 to 84 wt %. The LGP copolymers can be considered analogues of the commercially available amphiphilic triblock copolymers Pluronic, PEO–PPO–PEO, where PEO stands for poly(ethylene oxide), in which the flanking blocks of PEO are substituted by blocks of its structural analogue linear polyglycidol. In contrast to PEO, PG bears a hydroxyl group in each repeating monomer unit (Figure 1), which combined with its high biocompatibility<sup>3</sup> constitutes a potential platform for a variety of medical, pharmaceutical, biochemical, and biotechnological applications. It is remarkable that small alterations in the chemical structure of the hydrophilic blocks are manifested in significant differences in the aqueous solution properties compared to those of the corresponding Pluronic copolymers.<sup>1,2</sup> In general, the origin of the striking dissimilarities in the aqueous solution properties of the Pluronic and LGP copolymers can be attributed to the numerous hydroxyl groups that can promote strong hydrogen bonding. Both hydrophobic interactions via PPO and interactions via hydrogen bonding are considered equally involved in the formation of typically large aggregates. Another feature of the LGP copolymers is the well-documented

fact that the interactions of PPO and PG with water change in opposite manners upon heating, thus contrasting the well-known reverse solubility of both constituent blocks of the Pluronic copolymers. A number of distinct properties, e.g., lower cmc (critical micellization concentration) values, versatile cloud point behaviors, appearance of maxima and discontinuities in the temperature dependence of the aggregation number, anomalous thermotropic transitions, etc., have arisen from that feature.<sup>1,2</sup>

Besides, the relative molar mass of the middle block of PPO was also found to influence the self-assembly, dimensions, and aggregate structures of the LGP copolymers. For example, (i) LGP130 copolymers self-associate in aqueous solution easier (lower cmc values), however, their self-assembly is less temperature sensitive than that of LGP60 copolymers; (ii) the self-assembly for LGP130 is entropically less favored and the enthalpic barrier was further reduced compared to those of the related LGP60 copolymers; (iii) in strong contrast to LGP60 copolymers, LGP130 behave as non-Newtonian fluids in the dilute limit and are characterized by considerably higher magnitudes of the zero shear viscosity which is found to increase with increasing temperature; (iv) the concentrated solutions of LGP130 copolymers are invariably elastic at 60 °C and are typified by larger magnitudes of both moduli compared to those of LGP60 copolymers; (v) the copolymers of LGP130 series form denser and better defined particles and exhibit richer structural polymorphism as revealed by small-angle neutron scattering (SANS), dynamic and static light scattering (DLS and SLS), and cryogenic transmission electron microscopy studies.

The aim of the present article is to complement the systematic study on the family of LGP copolymers by creating a novel series

\*Corresponding author: Tel + 359 2 9792293, Fax + 359 2 8700309, e-mail Rangelov@polymer.bas.bg.

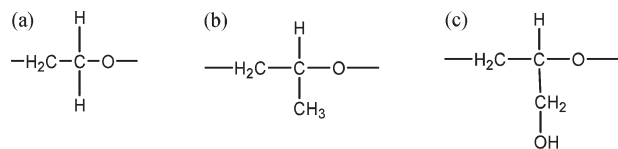


**Figure 1.** Monomer units of (a) poly(ethylene oxide), (b) poly(propylene oxide), and (c) linear polyglycidol.

of copolymers nominally based on PPO of molar mass of 1000 (hereinafter LGP30 copolymers) and investigating their aqueous solution properties. The PG content of the copolymers varies from 30 to 90 wt %, and thus they are closest in composition to the Pluronic series L31–F38. The aqueous solution properties in wide temperature and concentration intervals are investigated by determination of cmc, turbidimetry, rheology, and scattering methods. More specifically, we aim to explore the effect of the relative length (molar mass) of the central block of PPO by comparing properties of selected copolymers from the three (LGP30, LGP60, and LGP130) series.

## Experimental Section

**A. Materials.** The solvents (methanol, methylene chloride, tetrahydrofuran) were purified by distillation. Glycidol (96%, Aldrich) was distilled under reduced pressure. Ethyl vinyl ether (99%, Aldrich),  $\text{AlCl}_3 \cdot 6\text{H}_2\text{O}$  (99%, Aldrich), and  $\text{CsOH} \cdot \text{H}_2\text{O}$  (99.95%, Acros Organics) were used as received. Ethoxyethyl glycidyl ether (EEGE) was obtained by a reaction of glycidol and ethyl vinyl ether as described elsewhere.<sup>4</sup> Fractions of EEGE of purity exceeding 98.5%, determined by gas chromatography, were used for polymerization. Poly(propylene oxide) of molar mass 1000 corresponding to a degree of polymerization of 17 (Fluka) was dried by azeotropic distillation using toluene.

**B. Synthesis of Block Copolymers.** 1. *Preparation of the Macroinitiator.*  $\text{CsOH} \cdot \text{H}_2\text{O}$  (0.1343 g, 0.8 mmol) was added to PPO 1000 (0.5 g, 0.5 mmol) magnetically stirred at 90 °C in a reaction vessel equipped with argon and vacuum lines. After 2 h the reaction mixture was cooled to room temperature, and to remove the released water, 1 mL of dry benzene was added and vacuum was switched on for 2 h.

2. *Polymerization (Synthesis of PEEGE–PPO–PEEGE Precursors).* EEGE (3.95 g, 27 mmol) was introduced to the obtained macroinitiator to synthesize  $(\text{EEGE})_{27}(\text{PO})_{17}$  ( $(\text{EEGE})_{27}$ ). The polymerization was carried out in bulk at 90 °C. The conversion of the monomer was followed by  $^1\text{H}$  nuclear magnetic resonance spectroscopy ( $^1\text{H}$  NMR). The syntheses of the rest of the PEEGE–PPO–PEEGE precursors were carried out in analogy to this procedure.

3. *Deprotection Reaction (Synthesis of PG–PPO–PG Copolymers).* The procedure was adopted from a method for deprotection of tetrahydropyranyl ether, described elsewhere.<sup>5</sup> 3.29 g of  $(\text{EEGE})_{27}(\text{PO})_{17}(\text{EEGE})_{27}$ , containing 20 mmol of EEGE units, was dissolved in methanol (7.5 mL, 160 mmol).  $\text{AlCl}_3 \cdot 6\text{H}_2\text{O}$  (0.04 g, 0.2 mmol) was added, and the mixture was stirred for 1 h at room temperature. Afterward, the reaction product was filtered through Hyflo Super Gel (diatomaceous earth), and the solvents were evaporated under reduced pressure. The deprotection reactions for the rest of the copolymers were carried out analogously.

**C. Analysis.** 1. *Gel Permeation Chromatography (GPC).* The GPC analysis was carried out with a Waters system consisted of four Styragel columns with nominal pore sizes of 100, 500, 500, and 1000 Å and a refractive index detector R401. Tetrahydrofuran was used as an eluent at a flow rate of 1 mL/min at 40 °C. Samples were prepared as solutions in tetrahydrofuran. Toluene was used as the internal standard for indication of elution volume. Calibration was made with polystyrene standards.

2. *Turbidity Measurements.* The turbidity was determined by measuring the transmittance at  $\lambda = 500$  nm of aqueous solution

of the copolymers with concentrations ranging from 1 to 10 wt % at different temperatures using a Specord UV–vis spectrophotometer. The samples were placed in thermostated cuvette holder and heated slowly with heating rate of 1 °C/min from 20 to 85 °C. The temperature was controlled with accuracy of  $\pm 0.1$  °C.

3. *Determination of the Critical Micellization Concentration (cmc).* Aqueous solutions (2.0 mL) of a given triblock PG–PPO–PG copolymer in the concentration range from 0.001 to 5 wt % were prepared at 0 °C. 20  $\mu\text{L}$  of a 0.4 mM solution of 1,6-diphenyl-1,3,5-hexatriene (DPH) in methanol was added to each of the copolymer solutions. The solutions were incubated in the dark for 16 h at room temperature. The absorbance in the wavelength interval  $\lambda = 300$ –500 nm was followed at temperatures ranging from 40 to 60 °C on a Specord UV–vis spectrometer. The main absorption peak, characteristic for DPH solubilized in a hydrophobic environment, was at 356 nm.

4. *Rheology.* Oscillatory shear and steady shear experiments were carried out on a Thermo Haake 600 rheometer equipped with cone/plate and plate/plate geometry, respectively. The diameter and the gap width of the rotating inner bob were 60 and 2 mm, respectively, whereas the cone sensor diameter was 25 mm. Both series of experiments were carried out in a controlled stress mode. Copolymer solutions were transferred to the instrument and carefully overlaid with a low-viscosity silicone oil to minimize water evaporation. Oscillatory experiments were performed for high-viscosity samples (concentrated solutions). The storage modulus ( $G'$ ) and the loss modulus ( $G''$ ) were measured over the frequency range 0.01–1000 Hz. The values of the stress amplitude were checked in order to ensure that all measurements were performed within the linear viscoelastic region, where the dynamic moduli are independent of the applied stress. For low-viscosity samples (dilute solutions), steady shear experiments were performed in the range 0.01–2000  $\text{s}^{-1}$ . The measurements were performed at different temperatures ranging from 15 to 70 °C. The temperature was controlled with accuracy of  $\pm 0.1$  °C.

5. *Dynamic Light Scattering.* The light scattering setup has been described previously.<sup>6</sup> It consists of a 632.8 nm He/Ne laser and the detector optics with an ITT FW 130 photomultiplier and ALV-PM-PD amplifier–discriminator connected to an ALV-5000 autocorrelator built into a computer. The cylindrical scattering cells were sealed and then immersed in a large-diameter thermostated bath containing the index matching fluid decalin. Measurements were made at different angles in the range of 50°–130° and at different temperatures. Analysis of the dynamic data was performed by fitting the experimentally measured  $g_2(t)$ , the normalized intensity autocorrelation function, which is related to the electrical field correlation function  $g_1(t)$  by the Siegert relationship:<sup>7</sup>

$$g_2(t) - 1 = \beta |g_1(t)|^2 \quad (1)$$

where  $\beta$  is a factor accounting for deviation from ideal correlation. For polydisperse samples,  $g_1(t)$  can be written as the inverse Laplace transform (ILT) of the relaxation time distribution,  $\tau A(\tau)$ :

$$g_1(t) = \int \tau A(\tau) \exp(-t/\tau) d \ln \tau \quad (2)$$

where  $\tau$  is the lag time. The relaxation time distribution,  $\tau A(\tau)$ , was obtained by performing ILT using the constrained regularization algorithm REPES, which minimizes the sum of the squared differences between the experimental and the calculated  $g_2(t)$ .<sup>8</sup> A mean diffusion coefficient  $D$  was calculated from the position of each peak as  $D = \Gamma/q^2$ , where  $q$  is the magnitude of the scattering vector  $q = (4\pi n/\lambda) \sin(\theta/2)$  and  $\Gamma = 1/\tau$  is the relaxation rate of each mode. Here  $\theta$  is the scattering angle,  $n$  is

the refractive index of the medium, and  $\lambda$  is the wavelength of the light in a vacuum.

Within the dilute regime  $D$  varies linearly with the concentration according to

$$D = D_0(1 + k_D C + \dots) \quad (3)$$

where  $D_0$  is the diffusion coefficient at infinite dilution and  $k_D$  is the hydrodynamic virial coefficient. The Stokes–Einstein equation relates  $D_0$  and the hydrodynamic radius,  $R_h$ :

$$R_h = kT / (6\pi\eta D_0) \quad (4)$$

Here,  $kT$  is the thermal energy factor and  $\eta$  is the temperature-dependent viscosity of the solvent. Each data point reported here is an average of 4–6 separate measurements. The standard deviations were invariably smaller than the standard error of the method.

**6. Small-Angle Neutron Scattering.** The SANS data were collected at the SANS1 instrument at the FRG1 research reactor at GKSS Research Centre, Geesthacht, Germany.<sup>9</sup> The range of scattering vectors  $q$  from 0.005 to 0.26 Å<sup>-1</sup> was covered by four sample-to-detector distances (from 0.7 to 9.7 m). The neutron wavelength was 8.1 Å, and the wavelength spread of the mechanical velocity selector was 10% (fwhm). The samples were kept in quartz cells (Helma, Germany) with a path length of 1 mm. For isothermal conditions (10–60 °C), a thermostated sample holder was used. The raw spectra were corrected for backgrounds from the solvent, sample cell, and other sources by conventional procedures. The two-dimensional isotropic scattering spectra were azimuthally averaged, converted to absolute scale, and corrected for detector efficiency by dividing by the incoherent scattering spectrum of pure water, which was measured with a 1 mm path-length quartz cell. The smearing induced by the different instrumental settings was included in the data analysis.<sup>10</sup>

## Results

**Synthesis and Characterization of the Precursors and Targeting LGP30 Copolymers.** In order to obtain the novel LGP30 copolymers, the same two-step procedure as described earlier<sup>1a,2a</sup> was applied. First, PEEGE–PPO–PEEGE copolymer precursors were prepared by an anionic ring-opening polymerization of EEGE using partially deprotonated PPO 1000 as a macroinitiator. CsOH was used as a deprotonating agent, and all polymerizations were carried out in bulk at 90 °C. Then, the protective ethoxyethyl groups were cleaved, resulting in linear PG–PPO–PG copolymers. No destruction of the main backbone was observed during the deprotection.

GPC was utilized to prove the block structures of the copolymer precursors. GPC traces for the starting PPO 1000

and two of the resulting precursors are shown in Figure 2. The dispersity indices ranging from 1.12 to 1.36 were extracted from the data. The compositions of the precursors and targeting copolymers were determined from the <sup>1</sup>H nuclear magnetic resonance (<sup>1</sup>H NMR) data assuming an average degree of polymerization of the PPO moieties of 17. Representative spectra are shown in the Supporting Information. An excellent agreement between the degrees of polymerizations of the parent PEEGE blocks resulting PG blocks and theoretical values was found (Table 1).

**Aqueous Solution Properties.** The aqueous solutions properties of the novel LGP30 copolymers were studied in wide ranges of temperatures and concentrations by a number of experimental techniques including UV–vis spectroscopy, turbidimetry, light scattering, rheology, and small-angle neutron scattering. We start the section with determination of cmc and thermodynamics of the association.

**Cmc Determination and Thermodynamics of Association.** The properties of the nonpolar dye 1,6-diphenyl-1,3,5-hexatriene (DPH) were exploited to determine the cmcs as shown previously for various conventional and polymeric surfactants<sup>11</sup> as well as copolymers of the LGP60 and LGP130 series.<sup>1a,2a</sup> The appearance of a characteristic maximum at 356 nm in the absorption spectra of DPH is an indication of formation of hydrophobic domains in which the dye is solubilized. The cmcs were determined from the

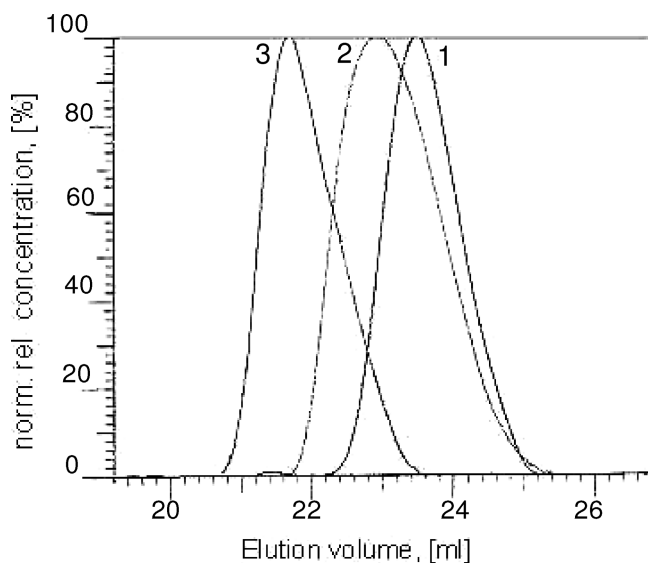


**Figure 2.** Gel permeation chromatography traces of starting PPO 1000 (1) and two copolymer precursors ((EEGE)<sub>27</sub>(PO)<sub>17</sub>(EEGE)<sub>27</sub> (2) and ((EEGE)<sub>61</sub>(PO)<sub>17</sub>(EEGE)<sub>61</sub> (3).

**Table 1. Targeting and Characterization Data of the Poly(ethoxyethyl glycidyl ether)–Poly(propylene oxide)–Poly(ethoxyethyl glycidyl ether) Precursors and Polyglycidol–Poly(propylene oxide)–Polyglycidol Block Copolymers**

total degree of polymerization of the flanking blocks					
targeting PG content (wt %)	theoretical	experimental		copolymer composition	abbreviation <sup>c</sup>
		PEEGE <sup>a</sup>	PG <sup>b</sup>		
30	6	6	6	(G) <sub>3</sub> (PO) <sub>17</sub> (G) <sub>3</sub>	LGP33
40	9	9	10	(G) <sub>5</sub> (PO) <sub>17</sub> (G) <sub>5</sub>	LGP34
50	14	12	12	(G) <sub>6</sub> (PO) <sub>17</sub> (G) <sub>6</sub>	LGP35
60	20	17	18	(G) <sub>9</sub> (PO) <sub>17</sub> (G) <sub>9</sub>	LGP36
70	31	26	28	(G) <sub>14</sub> (PO) <sub>17</sub> (G) <sub>14</sub>	LGP37
80	54	50	50	(G) <sub>25</sub> (PO) <sub>17</sub> (G) <sub>25</sub>	LGP38
90	122	120	124	(G) <sub>62</sub> (PO) <sub>17</sub> (G) <sub>62</sub>	LGP39

<sup>a</sup> Determined from the <sup>1</sup>H NMR spectra in CDCl<sub>3</sub>, assuming an average degree of polymerization of the middle PPO block of 17. <sup>b</sup> Determined from the <sup>1</sup>H NMR spectra in DMSO, assuming an average degree of polymerization of the PPO middle block of 17. <sup>c</sup> The last digit multiplied by 10 gives the PG content in wt %.



plot of DPH absorbance at 356 nm vs copolymer concentration, as shown in Figure 3a.

PPO is a thermosensitive polymer that exhibits lower critical solution temperature (LCST) properties in aqueous media.<sup>12</sup> In other words, upon heating it is able to undergo a temperature-induced phase separation from soluble to insoluble states. Particularly for PPO 1000, which serves as a middle block, LCST of about 35 °C is reported<sup>12c</sup> (see also experimental data in Figure 5), which means that no micellization below that temperature is expected. The cmc data for all copolymers studied are plotted as functions of temperature and PG contents in parts b and c of Figure 3, respectively. As seen from Table 1, the compositions of the copolymers LGP33, LGP34, and LGP35 are very close, and so are their cmcs. For the sake of simplicity the cmc data for these three copolymers are represented by that of LGP34. Generally, within the present series the same trends of the cmc variations with temperature and PG content as those for the relative copolymers of higher molecular weights (LGP60 and LGP130)<sup>1a,2a</sup> were observed. The variations, however, are somewhat less pronounced. In line with the expectations the cmc values of the copolymers of the present series are highest compared to those of the LGP60 and LGP130 series, which is demonstrated in Figure 3d for three composition analogues of the same (70 wt %) PG content at 40 °C. The LGP30 copolymers were found to self-associate easier (lower cmcs) than the corresponding Pluronic copolymers;<sup>13</sup> this counterintuitive feature has been repeatedly observed for the other two series.<sup>1a,2a</sup>

The thermodynamic parameters were extracted from the cmc data using eqs 5 and 6.

$$\Delta G^\circ = RT \ln(X_{\text{cmc}}) \quad (5)$$

$$\Delta G^\circ = \Delta H^\circ - T\Delta S^\circ \quad (6)$$

where  $\Delta G^\circ$  is the free energy of association,  $R$  is the gas law constant,  $T$  is the temperature in K,  $X_{\text{cmc}}$  is the cmc in mole fractions at temperature  $T$ , and  $\Delta H^\circ$  and  $\Delta S^\circ$  are the standard enthalpy and entropy of association, respectively.<sup>14</sup> The  $\Delta G^\circ$  values as a function of temperature for LGP36 are plotted in Figure 4. The negative values indicate spontaneous association, which is more favored at elevated temperatures (more negative values). Compared to the copolymers of the LGP60 and LGP130 series, however, the self-association of the copolymers of the present series is less favored (less negative values of  $\Delta G^\circ$ ), as clearly demonstrated in Figure 4 for representatives of the three groups. The values of  $\Delta H^\circ$  and  $\Delta S^\circ$  are collected in Table 2. Obviously, the self-association is an entropy-driven process. The positive entropy contributions, however, decrease with increasing PG content similarly to the rest of the LGP copolymers. The enthalpic barrier of the process is progressively reduced reaching only 1 J mol<sup>-1</sup> for LGP39.

**Turbidity Measurements.** The variations of the incident light intensity transmitted through semiconcentrated (1–10 wt %) solutions with temperature were monitored for the LGP30 copolymers. Representative transmittance vs temperature curves are shown in Figure 5; the clouding curve of an aqueous solution of PPO 1000 is also presented. The variations of the turbidity is strongly composition dependent (Figure 5). A typical clouding process presented by a sigmoidal curve is displayed by the copolymer of the lowest PG content, that is, LGP33. Compared to the clouding curve of PPO 1000, that of LGP33 is shifted to higher temperatures, and the cloud point at about 55 °C can be determined. The curve pattern changes drastically upon an increase in PG content by 10 wt %: the initially clear solution of LGP34

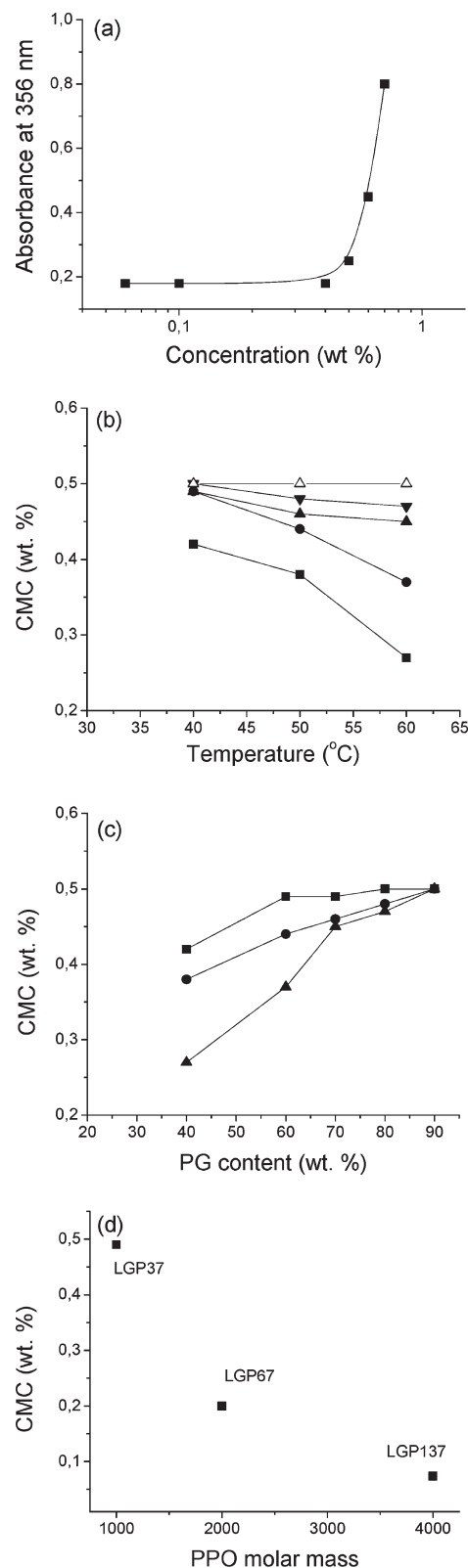


**Figure 3.** (a) Variations of the absorbance of DPH at 356 nm with LGP38 concentration at 40 °C. Critical micellization concentrations as a function of temperature (b) and PG content (c). Symbols in (b): LGP34 (squares); LGP36 (circles); LGP37 (triangles); LGP38 (inverted triangles); LGP39 (open triangles). Symbols in (c): 40 °C (squares); 50 °C (circles); 60 °C (triangles). (d) Variations of the critical micellization concentrations with the molar mass of the PPO block for three copolymers of 70 wt % PG content (LGP37, LGP67, LGP137) at 40 °C. The curves through the data points in (a), (b), and (c) are a guide for the eye.

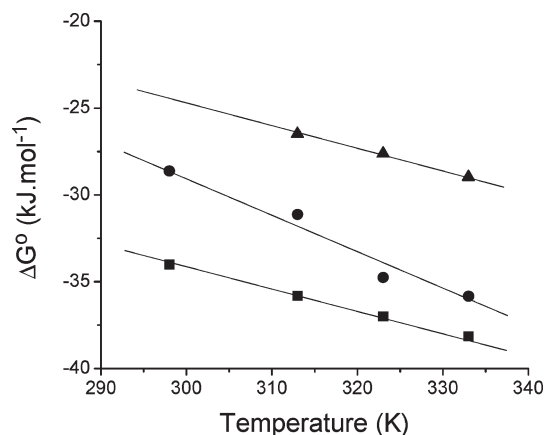


**Figure 4.** Free energy of association,  $\Delta G^\circ$ , as a function of temperature for LGP36 (triangles), LGP66 (circles), and LGP136 (squares). All copolymers have the same (60 wt %) PG content and differ in molar mass of the middle block of PPO. The lines through the data points are a guide for the eye.

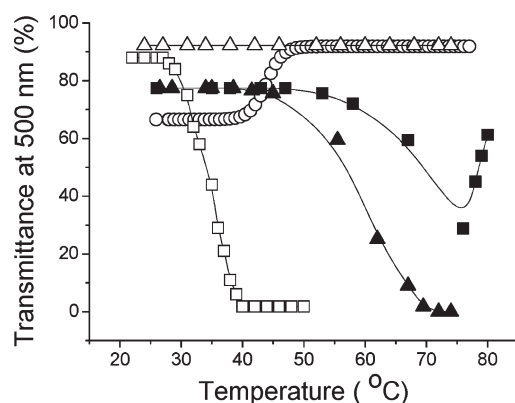


**Figure 5.** Transmittance vs temperature curves for aqueous solutions of PPO 1000 (open squares), LGP33 (closed triangles), LGP34 (closed squares), LGP35 (open circles), and LGP39 (open triangles). Concentrations 1 wt %.

**Table 2. Standard Enthalpy ( $\Delta H^\circ$ ) and Entropy ( $\Delta S^\circ$ ) of Association of the Investigated LGP30 Copolymers in Aqueous Solution**

copolymer	$\Delta H^\circ$ (kJ mol <sup>-1</sup> )	$\Delta S^\circ$ (kJ mol <sup>-1</sup> K <sup>-1</sup> )
LGP34	19.37	0.14
LGP36	12.36	0.12
LGP37	3.66	0.09
LGP38	2.71	0.09
LGP39	0.001	0.09

tends to cloud at a temperature that is further shifted to higher temperatures. However, clouding is not reached; instead, at certain temperature the transmittance sharply increases. For the copolymers of PG contents  $\geq 50$  wt % clouding is not observed. The curves are either reminiscent of materials exhibiting upper critical solution temperature properties (LGP35) or show no temperature variations (LGP36–LGP39). The abundance of curve patterns can be attributed to the varying in opposite manners interactions of PPO and PG with water upon heating.<sup>1a</sup> Most sensitive are the copolymers of intermediate PG contents which, correspondingly, display the most complicated behaviors.

**Dynamic Light Scattering.** Samples of aqueous dispersions were prepared in concentrations covering the 5.42–19.93 mg mL<sup>-1</sup> interval which is invariably above the cmcs (see above). The measurements were carried out at 40, 50, and 60 °C. Similarly to their composition analogues from the

LGP60 series,<sup>1b</sup> the present copolymers spontaneously form large particles. The relaxation time distributions of all samples, however, contained additional slow modes corresponding to particles with dimensions in the micrometer scale. An example of relaxation time distribution for LGP39 at 60 °C is presented in Figure 6a. Because of the unfavorable distributions, the static light scattering parameters were meaningless and therefore not presented. The attempts to get rid of the particles responsible for the slow modes were not successful: following filtration through appropriate pore size filters, the scattered light intensity of the dispersions dropped below the recommended minimum which prevented us from further investigations. Obviously, the large particles block part of the filter pores, and as a result, much of the material is filtered off. Fortunately, the slow modes were well separated from the dominant ones which made it possible to analyze the latter. Although the amplitudes of the dominant modes varied from sample to sample, they were typically above 75% of the overall scattered light intensity. A rough estimation of the ratio  $C_{\text{slow}}/C_{\text{dominant}}$  gives figures below 0.15. The routine procedure for determination of the dynamic parameters of the particles responsible for the dominant modes is presented in Figure 6b,c. The linear dependence of the relaxation rate,  $\Gamma$ , on  $\sin^2(\theta/2)$  passing through the origin indicates a diffusive process (Figure 6b). The diffusion coefficients were determined from the slopes of the linear fits and then plotted versus concentration to get the diffusion coefficient at infinite dilution,  $D_0$  (Figure 6c). The latter was used to calculate the hydrodynamic radii (eq 4), which are summarized in Table 3. As seen, the dominant particles are large. The data somewhat scatter, and typically no clear trends for the effects of either PG content or temperature on particle dimensions were observed. LGP33 is an exception in that respect; its particles tend to increase in size upon heating from 40 to 50 °C. In good agreement with turbidity measurements the dispersions become strongly opalescent at 60 °C. The hydrodynamic radii,  $R_h$ , were found to go through a maximum at intermediate PG contents. However, this is not a feature of the present series of copolymers: this phenomenon has been observed earlier for the composition analogues of higher molar mass, LGP60 and LGP130.<sup>1b,2b</sup> The feature of the LGP30 copolymers are the large dimensions of the particles they spontaneously form in aqueous solution. At equal PG content LGP30 copolymers invariably form larger in size aggregates than those of the LGP60 and LGP130 copolymers, which is demonstrated in Figure 6d for copolymers of PG contents of 70 wt %.

**Small-Angle Neutron Scattering Experiments.** SANS experiments were performed with concentrated (32.5 wt %) solutions of LGP38 and LGP39 at 15 and 60 °C. The SANS profiles for LGP39 are presented in Figure 7a. The scattering data were first analyzed by slope determination; the slopes at low ( $0.001\text{--}0.015\text{ \AA}^{-1}$ ) and large ( $>0.18\text{ \AA}^{-1}$ )  $q$  ranges were calculated and are summarized in Table 4. Strong scattering with slopes larger than 2.5 was observed at low  $q$ , which, in good agreement with the DLS data, is consistent with the presence of large particles. The significant scattering at intermediate and large  $q$  ranges indicates scattering from relatively small (few nanometers) structures, which might be PPO domains, loose clusters, and/or nonassociated copolymer chains. At large  $q$  the slopes invariably equaled 3.7, indicating the presence of an interface between the domains and the surrounding medium. The scattering curves were converted into real space equivalents, pair distance distribution function,  $p(r)$ , by applying a Pedersen's version<sup>15</sup> of the indirect Fourier transformation (IFT) procedure developed by Glatter.<sup>16</sup> IFT is a model-independent

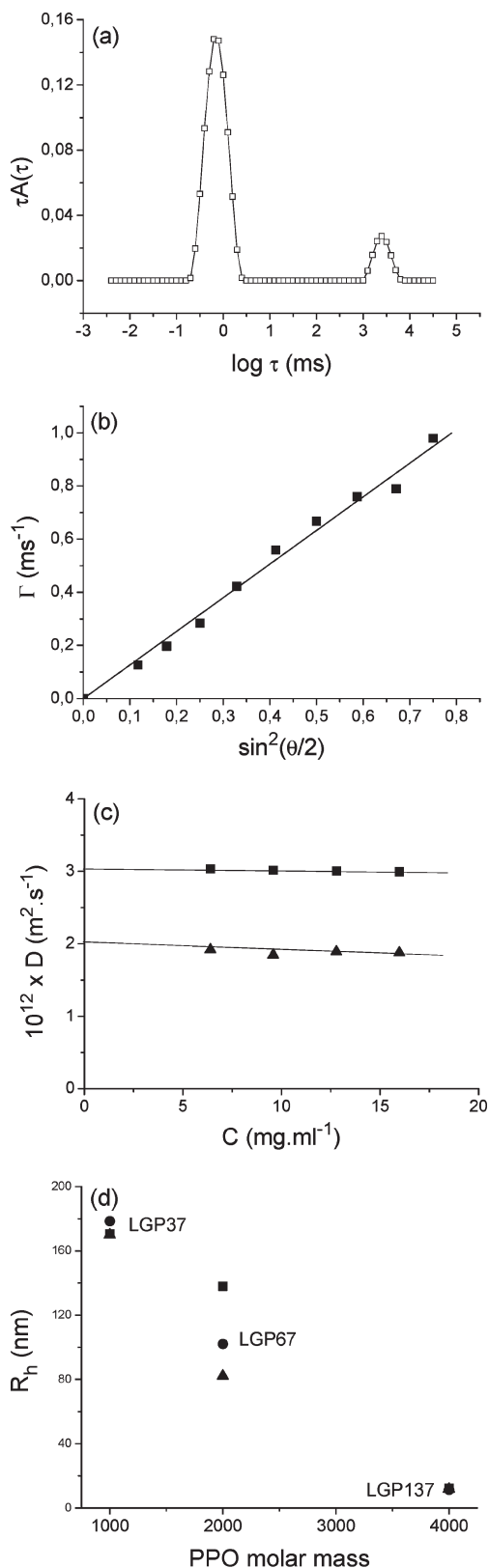


**Figure 6.** (a) An example of relaxation time distribution measured at an angle of  $90^\circ$  for an aqueous dispersion of LGP39 at  $7.97 \text{ mg mL}^{-1}$  and  $60^\circ\text{C}$ . (b) Relaxation rate,  $\Gamma$ , as a function of  $\sin^2(\theta/2)$  for LGP33 at  $c = 5.64 \text{ mg mL}^{-1}$  and  $40^\circ\text{C}$ . (c) Concentration dependence of the diffusion coefficients for LGP37 at  $40^\circ$  (triangles) and  $60^\circ\text{C}$  (squares). (d) Variations of  $R_h$  with the molar mass of the PPO block for three copolymers of 70 wt % PG content (LGP37, LGP67, LGP137) at  $40^\circ$  (squares),  $50^\circ$  (circles), and  $60^\circ\text{C}$  (triangles). The lines through the data points in (b) and (c) represent the linear fits to the data.

**Table 3.** Variations of the Hydrodynamic Radii,  $R_h$  (in nm), with Temperature for the Copolymers Studied in Water

copolymer	$40^\circ\text{C}$	$50^\circ\text{C}$	$60^\circ\text{C}$
LGP33	164.0	$270.0^a$	— <sup>b</sup>
LGP34	130.5	137.5	149.5
LGP36	1100	1300	1350
LGP37	170.5	178.5	170.0
LGP39	105.5	123.5	100.5

<sup>a</sup>Determined at a finite concentration of  $8.45 \text{ mg mL}^{-1}$ . <sup>b</sup>Milky-white opalescence.

approach requiring only a minimum of preliminary information for analysis, i.e., the maximum dimensions of the objects ( $D_{\text{max}}$ ). To obtain the size of the latter, the  $p(r)$  functions were calculated by (i) approximating the trace scattering from large particles to the power law  $q^{-\alpha}$  and (ii) assuming that the scattering structures are spherical 3D objects. As seen from Figure 7b, the  $p(r)$  functions are quite symmetrical, implying that the objects are almost spheres. The scattering at zero angle,  $I(0)$ , and the cross-sectional radius of gyration,  $R_g$ , were determined from the pair distance distribution functions; they are collected in Table 4. An interesting finding is that the dimensions of the scattering objects at 15 and  $60^\circ\text{C}$  are comparable being slightly larger at the elevated temperature. This is in strong contrast with the LGP60 copolymers studied earlier, for which a substantial increase in  $R_g$  values upon heating was observed.<sup>1c</sup> It has been suggested, however, that these are scattering objects of different composition being small size domains (predomains) with substantial contribution of PG and considerably larger domains dominated by PPO at lower and elevated temperatures, respectively.<sup>1c</sup> Analogously, we may expect the same type of behavior of LGP30 copolymers. Whereas the radii of gyration of the objects at  $15^\circ\text{C}$  for LGP60<sup>1c</sup> and LGP30 (Table 4) are very close, those at  $60^\circ\text{C}$  for LGP30 appear relatively small. However, considering the PPO molar mass and the enhanced solubility of the PG moieties at elevated temperatures, formation of large PPO domains cannot be expected. Figure 7c gives the size evolution of the PPO domains with molar mass of PPO for selected copolymers of LGP30, LGP60, and LGP130 series. The experimental findings are in line with the expectations.

The equivalent sphere radius,  $r$ , was calculated using eq 7. As seen from Table 4, the values of  $r$  are slightly below  $D_{\text{max}}/2$ , which implies slightly prolate shapes of the domains.

$$r = (5/3)^{1/2} R_g \quad (7)$$

The values of  $r$  were used to calculate the domain volumes,  $V$  (Table 4). Assuming that at  $60^\circ\text{C}$  the domains are entirely built by PPO and all PPO is in the domains, the aggregation number ( $N_{\text{agg}}$ ) can be estimated from the volume of the domains and the PPO volume ( $V_{\text{PPO}}$ ). The latter was calculated as the product  $17V_{\text{PO}}$ , where  $V_{\text{PO}}$  is the volume of the propylene oxide monomer unit ( $= 96.3 \text{ \AA}^3$ , see ref 17) and 17 is the polymerization degree of the PPO block. The results are collected in Table 4, whereas the evolution of the  $N_{\text{agg}}$  with PPO molar mass is presented in Figure 7d.

SANS was also used to study possible arrangements of the PPO domains into ordered structures. In contrast to the LGP copolymers based on longer PPO blocks, for which an arrangement compatible with a simple cubic phase was detected,<sup>1c</sup> no ordering for the LGP30 copolymers in the investigated concentration and temperature intervals was observed.

**Rheology of Aqueous Solutions.** In this section the molecular composition and aggregate structure are related with

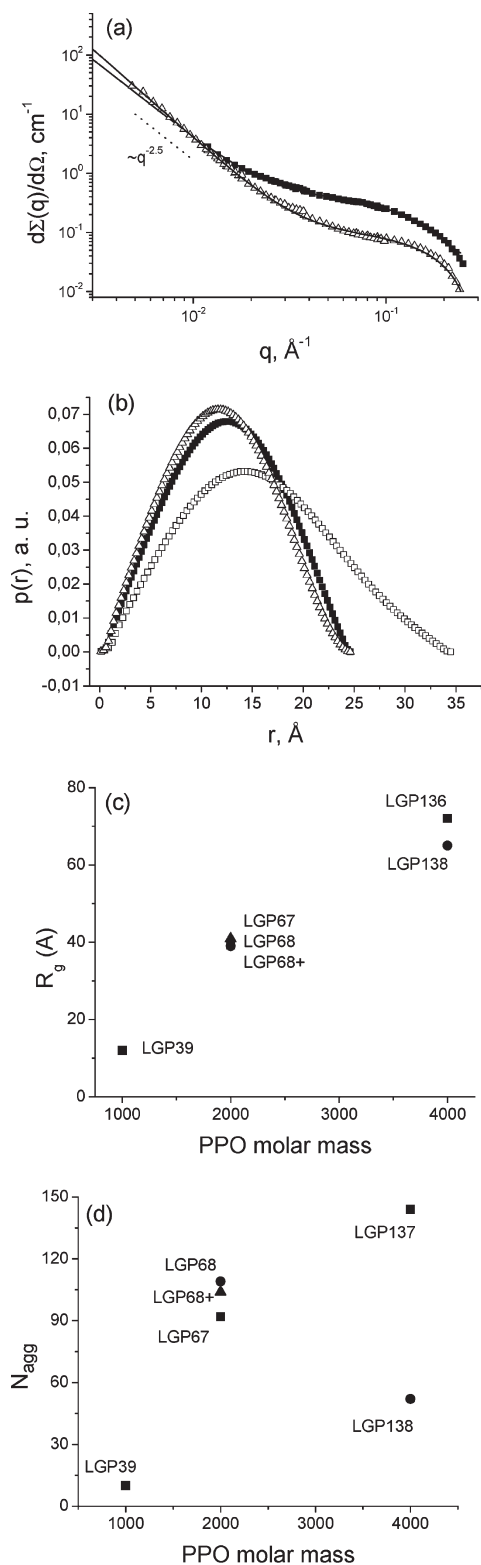


**Figure 7.** (a) SANS data for solution of LGP39 (32.5% in D<sub>2</sub>O) at 15 °C (triangles), 60 °C (squares), and corresponding model curves (solid lines) of IFT analysis with trace scattering of larger particles. Dashed line shows the slope of 2.5. (b) Pair distance distribution functions,  $p(r)$ , obtained from the SANS data of 32.5 wt % solutions in D<sub>2</sub>O of LGP38 at 15 °C (empty triangles), LGP39 at 15 °C (filled squares), and 60 °C (empty squares). (c) Variations of radii of gyration,  $R_g$ , of the PPO domains with the molar mass of the PPO block for selected copolymers of LGP30, LGP60, and LGP130 series in aqueous solution at 60 °C. (d) Variations of the aggregation number ( $N_{agg}$ ) of the PPO domains with the molar mass of the PPO block for selected copolymers of LGP30, LGP60, and LGP130 series in aqueous solution at 60 °C.

the rheological properties of the aqueous solutions of the LGP30 copolymers. Two concentration ranges were explored: dilute, up to 2 wt %, but invariably above the cmcs and concentrated, 33 wt %.

Steady shear viscosity measurements reveal that the solutions are Newtonian or exhibit very slightly a rheothining behavior typically in the upper concentration and temperature limits of the dilute range (Figure 8a). The rheothining is most pronounced for the solutions of LGP33 at 50 °C. This finding correlates very well with the proximity to the phase separation observed as clouding of the solution (see Figure 5) and the sharp increase in particle dimensions at that temperature (Table 3). The values of zero shear viscosity ( $\eta_0$ ) were obtained by extrapolation the viscosity curves to zero shear rate. With the exception of LGP33 at 50 °C,  $\eta_0$  is low ranging in the  $2.1 \times 10^{-4}$ – $1.6 \times 10^{-3}$  Pa·s interval. These values are orders of magnitude lower than those of the dilute solutions of LGP130 copolymers<sup>2a</sup> and comparable to those of LGP60 series,<sup>1d</sup> as demonstrated in Figure 8b for representatives of the three groups of copolymers containing 80 wt % of PG. The first impression is that the  $\eta_0$  values do not correlate with the data for particle dimensions (cf. Figures 6d and 8b). This counterintuitive observation, however, can be rationalized in terms of particles density and structure. It has been shown previously<sup>1b</sup> that the average density of the polymer material within the large compound particles that the LGP60 copolymers form is comparable to that of a flexible polymer coil in a good solvent. Obviously, the same or rather similar are the structure and density of the particles that the LGP30 copolymers form as emerging from the experimental data. That is why the macroscopic properties, in particular  $\eta_0$ , of these two series of copolymers are comparable in magnitude. In contrast, LGP130 copolymers form smaller but much more compact and denser particle that do not contain nonassociated chains,<sup>2b</sup> which is compatible with the considerably higher  $\eta_0$  values.<sup>2a</sup> Furthermore, the maximum in the particle dimensions at PG content of 60 wt % (Table 3) does not produce a pronounced maximum in the dependence of  $\eta_0$  on PG content. Here again the particle structure has a dominant role in governing the macroscopic properties: evidently, the particles that LGP36 forms although large are not dense and compact enough to cause appearance of a distinct maximum.

The concentrated ( $c = 33$  wt %) solutions were investigated by oscillatory experiments performed at a constant shear stress at temperatures ranging from 15 to 70 °C. With the exception of LGP33 which was found to phase separate at elevated temperatures, the behaviors of the rest of the copolymers are similar and differ in minor details. Therefore, data only for LGP39 that typifies the copolymers of the LGP30 series are presented. A representative mechanical spectrum showing frequency dependence of the storage ( $G'$ ) and loss ( $G''$ ) moduli is presented in Figure 9a. The frequency dependence is normally associated with the presence of lyotropic mesophases.<sup>18</sup> The spectra taken at 60 °C (Figure 9a) and 15 °C (not shown) practically overlap. At small deformation the solutions behave as viscous fluids with  $G'' > G'$ , whereas at frequencies above 3 Hz  $G'$  was found to rise above  $G''$ , indicating a predominant elastic character of the systems. Interestingly, compared to the copolymers of LGP60 and LGP130 series, the moduli curves of the concentrated solutions of the LGP30 copolymers are steeper and more frequency dependent.

At a given frequency and 60 °C the concentrated solutions invariably behave as fluids with low moduli values. Figure 9b shows nicely the differences with related LGP copolymers of higher both PPO block length and total molecular weight.



The rheological properties of the concentrated aqueous solutions were investigated during temperature sweeps 15–70–15 °C. The measurements were performed at a frequency of 0.04 Hz and a heating/cooling rate of 1 °C min<sup>-1</sup>. The results for the 33 wt % solution of LGP39 are shown in Figure 9c. The curve patterns of the concentrated solutions of the rest of the copolymers exhibit a general similarity. Invariably, the loss modulus is larger than the storage modulus, indicating that the solutions behave as fluids. A narrow interval of a sharp increase of both moduli was observed at about 35–40 °C, which coincided very well with the LCST of PPO 1000 and, in that aspect, can be associated with the formation of PPO domains. Crossovers, however, were not observed in the investigated temperature window, and the two curves went parallel to each other. During the cooling, the systems did not return to their initial state, which resulted in large hysteresis. The latter were observed for the related LGP60 copolymers<sup>1d</sup> as well as for some Pluronic copolymers.<sup>19</sup> Kinetic effects deriving from strong interparticle interactions are considered responsible

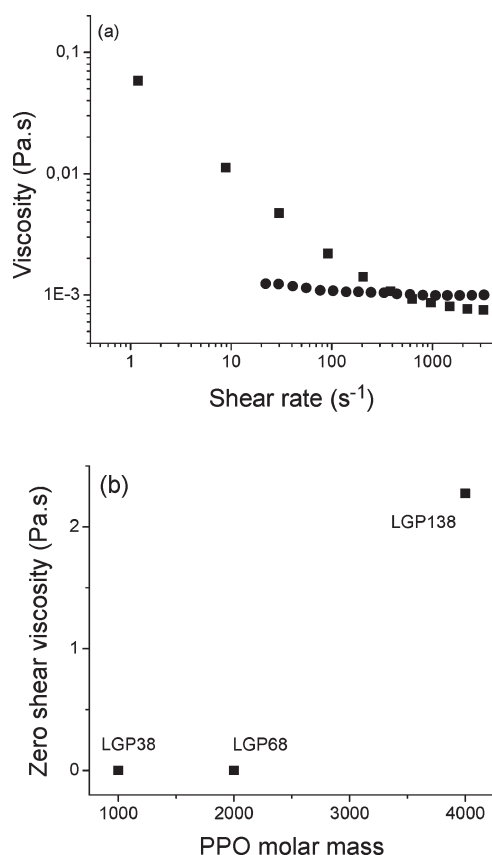


**Figure 8.** (a) Viscosity vs shear rate for 2.0 wt % solutions of LGP33 (squares) and LGP38 (circles) at 50 °C. (b) Variations of zero shear viscosity with the molar mass of the PPO block for three copolymers of 80 wt % PG content (LGP38, LGP68, LGP138) at 40 °C and concentration of 2 wt %.

for the hysteresis.<sup>1d,19</sup> In addition, the high viscosity of the solutions and the well-documented decrease of the solubility of PG upon decreasing temperature<sup>1a</sup> may also contribute to the hindered relaxation of the solutions. The retarded

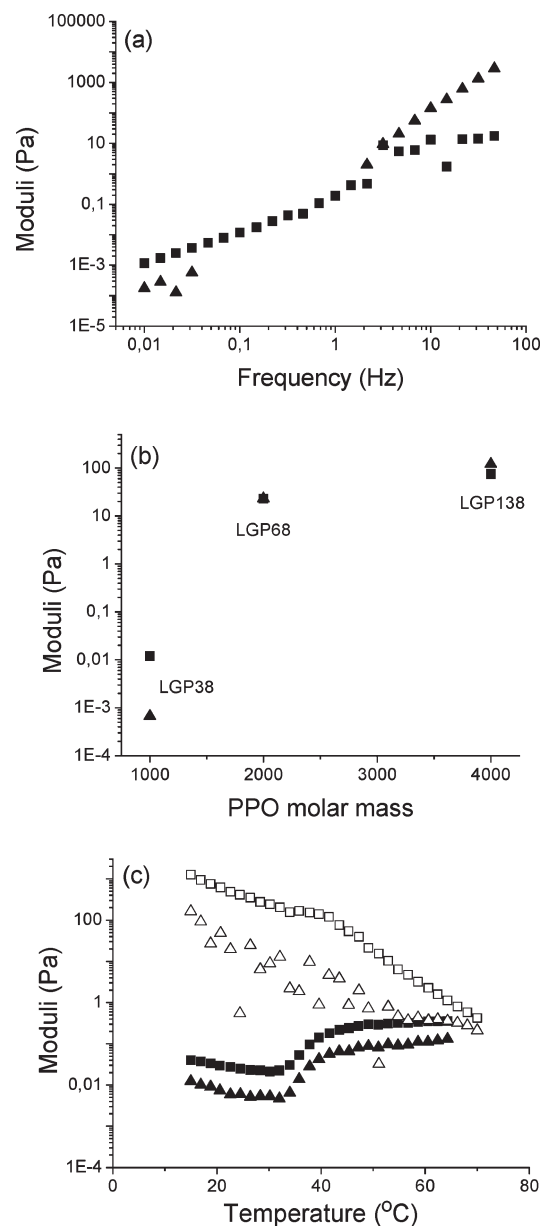


**Figure 9.** (a) Storage,  $G'$  (triangles), and loss,  $G''$  (squares), moduli as a function of frequency at 60 °C for a 33 wt % aqueous solution of LGP39. (b) Storage (triangles) and loss (squares) moduli as a function of PPO molar mass at a frequency of 0.1 Hz and temperature 60 °C, measured for 33 wt % aqueous solution of LGP38, LGP68, and LGP138. (c) Evolution of the storage (triangles) and loss (squares) moduli in the heating-cooling cycles for a 33 wt % aqueous solution of LGP39. Closed symbols: heating. Open symbols: cooling.

**Table 4.** Values of the Slopes Determined as  $I(q) \sim q^{-\alpha}$  at Different  $q$  Ranges, Cross-Sectional Scattering at Zero Angle ( $I(0)$ ), Cross-Sectional Radius of Gyration ( $R_g$ ), Finite Maximal Dimensions of the Domains ( $D_{\max}$ ), Equivalent Sphere Radius ( $r$ ), Volume ( $V$ ), and Aggregation Number ( $N_{\text{agg}}$ ) of the PPO Domains Formed in D<sub>2</sub>O by the Copolymers Studied

system	slopes at $q$ ranges		$I(0)$ (cm <sup>-1</sup> )	$R_g$ (Å)	$D_{\max}$ (Å)	$r$ (Å)	$V$ (Å <sup>3</sup> )	$N_{\text{agg}}$
	0.001–0.015	> 0.18						
LGP38, 15 °C	3.22	3.7	0.133	7.0	25.0	9.0	3050	10
LGP39, 15 °C	2.54	3.7	0.100	9.0	25.0	11.6	6500	
LGP39, 60 °C	2.58	3.7	0.370	12.0	35.0	15.5	15 600	



relaxation was further evidenced by the fact that the initial values of the moduli were reached after keeping the systems at 15 °C for hours.

## Discussion

In this paper a study on the synthesis and aqueous solution properties of a novel series of LGP copolymers (LGP30) that are close in composition to the Pluronic copolymers of the lowest molar mass of the central block of PPO, L31–F38, is reported. The copolymers are nominally based on PPO of molar mass of 1000, which allows direct comparison of their properties with those of copolymers from other series of LGP copolymers, LGP60<sup>1</sup> and LGP130,<sup>2</sup> that are nominally based on PPO of molar masses of 2000 and 4000, respectively. Whereas in the previous papers<sup>1,2</sup> the emphasis has been put mainly on the effect of substitution of the PEO blocks by linear PG and the influence of PG content on the aqueous solution properties, in the present contribution by exploring properties of the LGP30 copolymers and comparing them to those of LGP60 and LGP130 copolymers, we tried to achieve a better understanding of the role of the constituent blocks and, in particular, the influence of the relative molar mass of the central block of PPO.

It can be concluded that the LGP30 copolymers to a large extent follow the common rules of behavior exhibited by the LGP60 copolymers<sup>1</sup> and differ only in (minor) details. The differences are larger as far as the LGP130 copolymers<sup>2</sup> are concerned. Owing to the specificity of the central block exhibiting LCST of about 35 °C,<sup>12c</sup> no association driven by hydrophobic interactions was observed at temperatures below 35 °C. Above that temperature the LGP30 copolymers spontaneously self-associate ( $\Delta G^\circ < 0$ ), but compared to their composition analogues, LGP60 and LGP130, the association process is less favored as evidenced by the invariably higher cmcs (Figure 3d) and less negative  $\Delta G^\circ$  values (Figure 4). The central block, PPO of molar mass of 1000, which is the most hydrophilic among the central blocks of the copolymers of series LGP60 and LGP130, is considered responsible for the less favored self-association of the LGP30 copolymers. The slight temperature dependence of cmc is a feature of all copolymers from the LGP family and can be attributed to the specificity of polyglycidol: its solubility in water increases with increasing temperature, which compensates to a large extent the enhanced hydrophobicity of the PPO moieties.

Similarly to the copolymers of the other two series, the variations of turbidity of semiconcentrated solutions of LGP30 copolymers with temperature are strongly composition dependent with the most eventful curve patterns observed for the copolymers with intermediate PG contents (Figure 5). Somewhat complicated curve patterns (e.g., two cloud points) have been occasionally reported for Pluronic copolymers<sup>20</sup> and attributed to the presence of hydrophobic impurities. This trivial explanation has been ruled out since the copolymers are adequately purified; it is considered that the delicate balance between the constituent blocks whose solubility in water changes with temperature in an opposite fashion is behind the abundance of curve patterns.

The particles that the LGP30 copolymers form are quite similar to those formed by the LGP60 copolymers. These are large compound particles consisting of discontinuous domains built of PPO, which are dispersed in a considerably less compact medium containing individual copolymer chains and water that extends itself continuously throughout the whole particle as revealed by the combined light scattering and SANS studies. At all PG contents the particles of LGP30 copolymers are larger than those of the corresponding LGP copolymers as nicely demonstrated in Figure 6d. The large compound particles of the LGP30 copolymers are, however, somewhat less defined in

terms of coexistence with micrometer-sized particles and dimensions of the PPO domains. On the basis of previous experience<sup>1b,2b</sup> and considering the slight hydrophobic nature of the central block of the LGP30 copolymers, a model of the particle structure resembling emulsion droplets is in line with the expectations.

The evolutions of both dimensions ( $R_g$ ) of the PPO domains and their aggregation number derived from the SANS experiments were analogous to those of the Pluronic copolymers.<sup>21</sup> The evolutions are seemingly governed by the PPO block molar mass (Figure 7c,d); however, the effect of the hydrophilic, that is PG, blocks, the proximity of the temperature interval studied to the LCST of PPO blocks, and the molar mass dependent hydrophobicity of the latter are also contributing factors.

Although the particles of LGP30 are larger than those of the composition analogues, the dilute solutions, with very few exceptions, behave as Newtonian fluids and exhibit zero shear viscosity values that are comparable to and orders of magnitude lower than those of the dilute solutions of LGP60<sup>1d</sup> and LGP130,<sup>2a</sup> respectively (see Figure 8b). The larger dimensions are obviously not able to produce a sharp increase in zero shear viscosity and transitions to non-Newtonian behavior most probably because the particles are not dense and compact enough. For the concentrated solutions the loss modulus was found to be invariably larger than the storage modulus, thus contrasting the concentrated solutions of LGP60 and LGP130 copolymers for which crossovers, that is sol–gel transitions, and large gel regions in the phase diagrams have been observed.<sup>1d,2a</sup> Generally, it can be said that the large hystereses observed in the heating–cooling cycles and retarded relaxation are typical for both LGP<sup>1d,2a</sup> and Pluronic copolymers of higher molar mass of the PPO block and PEO content.<sup>19</sup>

Similarly to their closest Pluronic analogues (L31–F38), the LGP30 copolymers are not expected to exhibit pronounced ability to form gels and impressive performance of the latter. In fact, even at concentrations and temperatures as high as 33 wt % and 60 °C, they behave as viscous fluids. The effect of increasing PPO block length on the values of the moduli is demonstrated in Figure 9b. It clearly shows also the transitions from a nonelastic to elastic behavior of the solutions. It should be noted here that the longer PG chains and the increased total molecular weight have also contributed to the moduli variations and nonelastic to elastic transitions.

## Conclusions

A series of seven polyglycidol containing triblock PG–PPO–PG copolymers were prepared by applying a two-step synthetic procedure. The novel copolymers (LGP30) are closest in composition to the Pluronic series L31–F38: they are based on PPO of molar mass of 1000, whereas the PG content ranges from 30 to 90 wt %. Their aqueous solution properties were investigated by determination of the cmcs, turbidimetry, and rheology; the particles that are formed above certain critical concentration or temperature were parametrized by scattering (DLS and SANS) methods. By designing precisely the compositions of the LGP30 copolymers and comparing their properties with those of related copolymers studied earlier—LGP60 and LGP130 which are based on PPO of molar masses of 2000 and 4000, respectively<sup>1,2</sup>—it was possible to explore the role of the relative length (molar mass) of the middle block of PPO. The self-association process of the LGP30 copolymers is obviously less favored judging from the highest cmcs and less negative  $\Delta G^\circ$  values. At all PG contents and temperatures studied the particles that LGP30 copolymers form are largest in size and least defined compared to the nanostructures formed by LGP60 and LGP130 copolymers. In contrast, the discontinuous PPO domains inside the large compound particles are characterized by the lowest radii of gyration and aggregation numbers. The specific structure of

the particles governs the rheological properties of the LGP30 copolymers which are typified by invariably lowest zero shear viscosity values and behavior as viscous fluids even at concentrations and temperatures as high as 33 wt % and 60 °C.

**Acknowledgment.** The financial support from the National Science Fund of Bulgaria (Contract DO 02-247/18.12.2008) and the COST programme (COST-STSM-P12-02727) is gratefully acknowledged. The SANS measurements were supported by the European Commission under the sixth Framework Programme through the Key Action: Strengthening the European Research Area, Research Infrastructures (Contract RII3-CT-2003-505925). The donation of Alexander von Humboldt Stiftung and the Bulgarian Academy of Sciences to purchase the rheometer Thermo Haake 600 is gratefully acknowledged.

**Supporting Information Available:**  $^1\text{H}$  NMR spectra of  $(\text{EEGE})_6(\text{PO})_{17}(\text{EEGE})_6$  in  $\text{CDCl}_3$ ,  $(\text{G})_6(\text{PO})_{17}(\text{G})_6$  in  $\text{D}_2\text{O}$ , and  $(\text{G})_{62}(\text{PO})_{17}(\text{G})_{62}$  in DMSO. This material is available free of charge via the Internet at <http://pubs.acs.org>.

## References and Notes

- (1) (a) Halacheva, S.; Rangelov, S.; Tsvetanov, Ch. *Macromolecules* **2006**, *39*, 6845–52. (b) Rangelov, S.; Almgren, M.; Halacheva, S.; Tsvetanov, Ch. *J. Phys. Chem. C* **2007**, *111*, 13185–91. (c) Halacheva, S.; Rangelov, S.; Garamus, V. *Macromolecules* **2007**, *40*, 8015–21. (d) Halacheva, S.; Rangelov, S.; Tsvetanov, Ch. *J. Phys. Chem. B* **2008**, *112*, 1899–905.
- (2) (a) Halacheva, S.; Rangelov, S.; Tsvetanov, Ch. *Macromolecules* **2008**, *41*, 7699–705. (b) Rangelov, S.; Halacheva, S.; Garamus, V.; Almgren, M. *Macromolecules* **2008**, *41*, 8885–94.
- (3) Kainthan, R. K.; Janzen, J.; Levin, E.; Devine, D. V.; Brooks, D. E. *Biomacromolecules* **2006**, *7*, 703–9.
- (4) Fitton, A.; Hill, J.; Jane, D.; Miller, R. *Synthesis* **1987**, 1140–2.
- (5) Namboodri, V. V.; Varma, R. S. *Tetrahedron Lett.* **2002**, *43*, 1143–6.
- (6) Rangelov, S.; Brown, W. *Polymer* **2000**, *41*, 4825–30.
- (7) Chu, B. In *Laser Light Scattering*; Academic Press: New York, 1991; Vol. 2.
- (8) Jakes, J. *Czech J. Phys. B* **1988**, *38*, 1305–16.
- (9) Stuhmann, H. B.; Burkhardt, N.; Dietrich, G.; Junemann, R.; Meerwinck, W.; Scmitt, M.; Wadzak, J.; Willumeit, R.; Zhao, J.; Nierhaus, K. H. *Nucl. Instrum. Methods* **1995**, *A356*, 133.
- (10) Pedersen, J. S.; Posselt, D.; Mortensen, K. *J. Appl. Crystallogr.* **1990**, *23*, 321.
- (11) (a) Alexandridis, P.; Holzwarth, J. F.; Hatton, T. A. *Macromolecules* **1994**, *27*, 2414–25. (b) Chattopadhyay, A.; London, E. *Anal. Biochem.* **1984**, *139*, 408–12. (c) Svensson, M.; Linse, P.; Tjerneld, F. *Macromolecules* **1995**, *28*, 3597–603. (d) Scherlund, M.; Brodin, A.; Malmsten, M. *Int. J. Pharm.* **2000**, *211*, 37–49. (e) Rangelov, S.; Petrova, E.; Berlinova, I.; Tsvetanov, Ch. *Polymer* **2001**, *42*, 4483–91.
- (12) (a) Malmsten, M.; Linse, P.; Zhang, K.-W. *Macromolecules* **1993**, *26*, 2905. (b) Mortensen, K.; Schwahn, D.; Janssen, S. *Phys. Rev. Lett.* **1993**, *71*, 1728. (c) Schild, H. G.; Tirell, D. A. *J. Phys. Chem.* **1990**, *94*, 4352. (d) Dimitrov, Ph.; Rangelov, S.; Dworak, A.; Tsvetanov, Ch. *Macromolecules* **2004**, *37*, 1000–8.
- (13) (a) Wanka, G.; Hoffmann, H.; Ulbricht, W. *Macromolecules* **1994**, *27*, 4145–59. (b) Lopes, J. R.; Loh, W. *Langmuir* **1998**, *14*, 750–6.
- (14) Hunter, R. J. *Foundations of Colloid Science*; Oxford University Press: New York, 1987; Vol. 1.
- (15) Pedersen, J. S. *Adv. Colloid Interface Sci.* **1997**, *70*, 171–210.
- (16) Glatte, O. J. *J. Appl. Crystallogr.* **1977**, *10*, 415–21.
- (17) Mortensen, K. *Colloids Surf., A* **2001**, *183*, 277–92.
- (18) Hamley, I. W. *The Physics of Block Copolymers*; Oxford University Press: New York, 1998.
- (19) Lau, B. K.; Wang, Q.; Sun, W.; Li, L. *J. Polym. Sci., Part B: Polym. Phys.* **2004**, *42*, 2014.
- (20) (a) Desai, P. R.; Jain, N. J.; Bahadur, P. *Colloids Surf., A* **2002**, *197*, 19–26. (b) da Silva, R. C.; Loh, W. J. *Colloid Interface Sci.* **1998**, *202*, 385–9. (c) Zhou, Z.; Chu, B. *Macromolecules* **1988**, *21*, 2548–54.
- (21) Nagarajan, R.; Ganesh, K. *Macromolecules* **1989**, *22*, 4312–25.